

Hierarchical Data-efficient Representation Learning for Tertiary Structure-based RNA Design

Cheng Tan^{1,5*}, Yijie Zhang^{2*}, Zhangyang Gao^{1,5}, Hanqun Cao^{3,4} and Stan Z. Li^{5†}

¹Zhejiang University, ²McGill University, ³The Chinese University of Hong Kong, ⁴Zhejiang Lab

⁵AI Lab, Research Center for Industries of the Future, Westlake University
{tancheng, gaozhangyang, stan.zq.li}@westlake.edu.cn

Abstract

While artificial intelligence has made remarkable strides in revealing the relationship between biological macromolecules' primary sequence and tertiary structure, designing RNA sequences based on specified tertiary structures remains challenging. Though existing approaches in protein design have thoroughly explored structure-to-sequence dependencies in proteins, RNA design still confronts difficulties due to structural complexity and data scarcity. Adding to the problem, direct transplantation of protein design methodologies into RNA design fails to achieve satisfactory outcomes although sharing similar structural components. In this study, we aim to systematically construct a data-driven RNA design pipeline. We crafted a large, well-curated benchmark dataset and designed a comprehensive structural modeling approach to represent the complex RNA tertiary structure. More importantly, we proposed a hierarchical data-efficient representation learning framework that learns structural representations through contrastive learning at both cluster-level and sample-level to fully leverage the limited data. By constraining data representations within a limited hyperspherical space, the intrinsic relationships between data points could be explicitly imposed. Moreover, we incorporated extracted secondary structures with base pairs as prior knowledge to facilitate the RNA design process. Extensive experiments demonstrate the effectiveness of our proposed method, providing a reliable baseline for future RNA design tasks. The source code and benchmark dataset will be released publicly.

1 Introduction

Ribonucleic acid (RNA) is a fundamental polymer composed of ribonucleotides, serving as a vital biological macromolecule that regulates a plethora of cellular functions [45, 35, 72, 87]. Non-coding RNA strands exhibit intricate three-dimensional structures, which are essential for their biological activities [21, 34]. The complex geometries of RNA molecules empower them to execute irreplaceable functions in crucial cellular processes [15], encompassing but not limited to mRNA translation [65], RNA splicing [67, 86, 48], and gene regulation [54, 18, 83].

Specifically, the primary structure of RNA refers to its linear sequence of ribonucleotides. The primary structure then folds into a secondary structure with canonical base pairs, forming stems and loops. Tertiary interactions between secondary structural elements subsequently give rise to the three-dimensional structure. Figure 1 illustrates an example of the hierarchical folding of RNA primary, secondary, and tertiary structures. Gaining a comprehensive understanding of RNA structure is fundamental to unraveling biological mysteries and holds tremendous promise for biomedical

*Equal contribution.

†Corresponding author.

applications. However, solving RNA structures through experimental techniques remains challenging due to their structural complexity and transient nature. Computational modeling of RNA structure and dynamics has thus become particularly valuable and urgent.

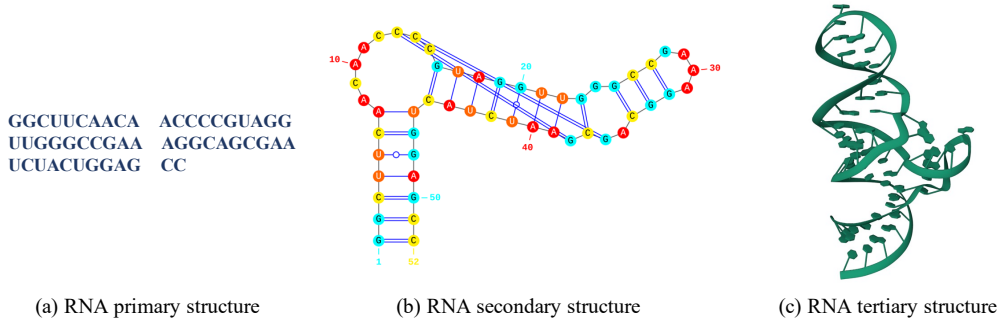


Figure 1: The schematic diagrams of RNA primary, secondary and tertiary structures.

Recent years have witnessed the emergence and rapid advancement of data-driven computational modeling of RNA [3, 91, 71]. In particular, algorithms for RNA secondary structure prediction have been extensively developed, yielding impressive results through leveraging large datasets of known secondary structures [70, 13, 23, 74]. However, knowledge of RNA tertiary structures, which is crucial for thoroughly understanding RNA functional mechanisms and discovering RNA-targeted therapies [87, 14], remains limited [81]. The success of protein structure prediction approaches [43, 4] has motivated researchers to tackle the even more challenging problem of RNA tertiary structure prediction, leading to the development of RNA tertiary structure folding algorithms such as DeepFoldRNA [60], RoseTTAFoldNA [5], and RhoFold [11, 69]. While predicting RNA tertiary structures from primary sequences can leverage abundant sequence data [11], its inverse problem, designing RNA sequences that reliably fold into a specified tertiary structure, remains largely underexplored.

The key reasons that RNA tertiary structure modeling lags far behind protein tertiary structure modeling stem from two main aspects: (1) RNA demonstrates greater structural intricacy and flexibility than proteins, posing formidable hurdles for structure prediction and design [81, 8, 7]. The less constrained structure space of RNA leads to intractable challenges in modeling the RNA tertiary structure. (2) High-resolution RNA tertiary structures are scarce compared to proteins due to their conformational dynamics and instability [6, 66]. The quantity of available RNA structures constitutes less than 1% of that for proteins [1, 44]. To deal with the above problem, we propose a thorough pipeline aiming at data-driven tertiary structure-based RNA design tasks. In detail, we first compile a large-scale RNA tertiary structure dataset based on extant high-quality structure data from Protein Data Bank (PDB) [6, 7] and RNAsolo [1]. Then, regarding the deficiency in effective RNA tertiary structure modeling methods and the unsatisfying transferable capability of conventional protein structure modeling techniques to the RNA field, we propose a comprehensive RNA tertiary structure modeling approach. To optimize the use of the limited data, we introduce a hierarchical and data-efficient representation learning framework that applies contrastive learning at both the cluster and sample levels. In this way, we can explicitly impose intrinsic relationships between the data by constraining the data representations within a limited hyperspherical space. Moreover, we provide a strategy that utilizes extracted secondary structure as prior information to guide the RNA design inspired by the correlation between RNA secondary and primary structures.

The main contributions of this work are summarized as follows:

- We propose a formal formulation of the tertiary structure-based RNA design problem. To establish a fair benchmark for tertiary structure-based RNA design, we compile a large dataset of RNA tertiary structures and provide a fundamental data split based on both structural similarity and sequence length distribution.
- We propose a comprehensive structural modeling approach for representing the complex RNA tertiary structure. Based on that, we design a RNA design framework called *RDesign*, which is composed of a hierarchical representation learning scheme and a secondary structure imposing strategy. Specifically, the hierarchical scheme learns from limited data in a data-efficient manner and the strategy incorporates extracted secondary structures as prior knowledge to facilitate the RNA design process.

- Through extensive experiments across standard RNA design benchmarks and generalization ability assessments, we have conclusively demonstrated the efficacy of our proposed method. This provides a reliable pipeline for future research in this important and promising field.

2 Related work

2.1 Biomolecular Engineering

In recent decades, the rapid advancements in artificial intelligence [80, 73, 75, 31, 78, 100, 98, 99, 10], biophysics, biochemistry [29, 25, 28, 90, 30, 88], and chemical engineering [89] have resulted in a plethora of novel applications [56, 76, 77, 39, 92], including engineering enzymes for industrial biocatalysis [61], tailoring antibodies for precision cancer therapies [41], developing trackable fluorescent proteins for biological imaging [64], and optimizing polymerases for forensic DNA analysis [52]. RNA design is of particular interest among them due to the diverse functions that RNA can fulfill, ranging from translation and gene expression to catalysis [20]. This multifunctionality is ascribed to the structural diversity of RNA [2]. In this work, we focus on tertiary structure-based RNA design to uncover the relationships between RNA structure and sequence.

2.2 Protein Design

RNA and protein are essential components of cells. Despite having different chemical constituents, their higher-order structures can be described similarly [66]. Therefore, they also share some functioning principles. Early works on computational protein design [49, 59, 84, 12] utilize multi-layer perceptron (MLP), convolutional neural network (CNN) to predict residue types from protein structure. 3D CNNs have enabled tertiary structure-based design such as ProDCoNN [96] and DenseCPD [62]. GraphTrans [40] combines attention [82] and auto-regressive decoding to generate protein sequences from graphs, inspiring series of recent advancing approaches [42, 79, 17, 38, 26, 27]. While insights from protein research have illuminated RNA biology, RNA studies have trailed due to a paucity of available data and complex structure modeling [24].

2.3 RNA Design

The computational design of RNA sequences aims to generate nucleic acid strands that will fold into a targeted secondary or tertiary structure. Secondary structure-based RNA design was first introduced by Vienna [37]. Early works solved the RNA design problem through stochastic optimization and energy minimization with thermodynamic parameters, such as RNAfold [36, 51], Mfold [101], UNAFold [58], and RNAstructure [53]. Probabilistic models and posterior decoding were also employed to solve this problem [47, 68]. Local search strategies mutate the seed RNA sequence and repeatedly minimize energy to predict RNA folding. The objective is to find a designed sequence with desired folding properties using an optimization problem formulation [14]. Other works that operate on a single sequence and try to find a solution by changing a small number of nucleotides include RNAInverse [37], RNA-SSD [2], INFO-RNA [9], and NUPACK [95]. There are also global searching methods, including antaRNA [46] and MCTS-RNA [93]. Reinforcement learning-based methods have also been developed [19, 67].

Although numerous approaches have been studied for engineering RNA secondary structures, RNA design based on the tertiary structure is still challenging due to the lack of high-resolution structural data [94, 16]. Although structure prediction algorithms [50, 63, 85] can utilize abundant RNA primary sequence information, the progress of RNA design has been hindered by the scarcity of determined RNA 3D structures. To alleviate the difficulty, we explore the uncharted areas of tertiary structure-centric RNA design systematically and propose a complete pipeline to address this challenge.

3 Method

3.1 Preliminaries

For an RNA sequence in its primary structure, we assume it comprises N nucleotide bases selected from the set of nucleotides: A (*Adenine*), U (*Uracil*), C (*Cytosine*), and G (*Guanine*). Therefore, the

sequence can be represented as:

$$\begin{aligned} \text{Nucleotides} &:= \{A, U, C, G\}, \\ \mathcal{S}^N &= \{s_i \in \text{Nucleotides} \mid i \in [1, N] \cap \mathbb{Z}\}, \end{aligned} \quad (1)$$

The formation of the tertiary structure requires the folding of this sequence in three-dimensional space, which can be denoted as:

$$\begin{aligned} \text{Atoms} &:= \{P, O5', C5', C4', C3', O3'\}, \\ \mathcal{X}^N &= \{\mathbf{x}_i^\omega \in \mathbb{R}^3 \mid i \in [1, N] \cap \mathbb{Z}, \omega \in \text{Atoms}\}, \end{aligned} \quad (2)$$

where the Atoms set denotes the six atoms that comprise the RNA backbone.

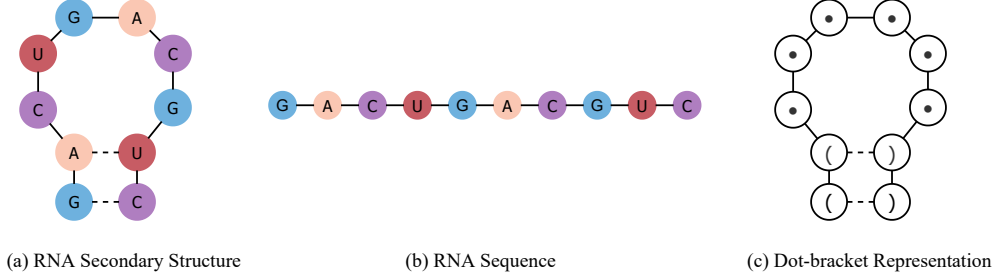


Figure 2: Brief view of RNA sequence and secondary structure.

We also incorporate secondary structure information by using dot-bracket notation. In this notation, unpaired nucleotides are represented by dots, and paired nucleotides are represented by brackets, as shown in Figure 2.

$$\mathcal{A}^N = \{a_i \in \{., (,), \} \mid i \in [1, N] \cap \mathbb{Z}\}, \quad (3)$$

where a_i is a dot if the nucleotide is unpaired, or a matching bracket otherwise. Finally, the tertiary structure-based RNA design problem could be formulated as:

$$\begin{aligned} \mathcal{F}_\Theta : \mathcal{X}^N &\mapsto \mathcal{S}^N, \\ \text{such that } \mathcal{A}^N &= g(\mathcal{S}^N) = g(\mathcal{F}_\Theta(\mathcal{X}^N)), \end{aligned} \quad (4)$$

where \mathcal{F}_Θ is a learnable mapping with parameters Θ , and $g(\cdot)$ is a function that extracts the secondary structure from the tertiary structure.

3.2 Comprehensive RNA Tertiary Structure Modeling

We first construct a local coordinate system Q_i for the i -th nucleotide in the RNA tertiary structure. The detailed procedure for defining the local coordinate system is elucidated in Appendix ?? . While studies on protein design have achieved considerable success using only the $C\alpha$ atoms to model backbone geometry, this approach does not readily translate to RNA. RNA exhibits a diversity of backbone conformations and base-pairing geometries that cannot be sufficiently captured by such modeling approaches. The complexity and plasticity of RNA structure necessitate a comprehensive treatment.

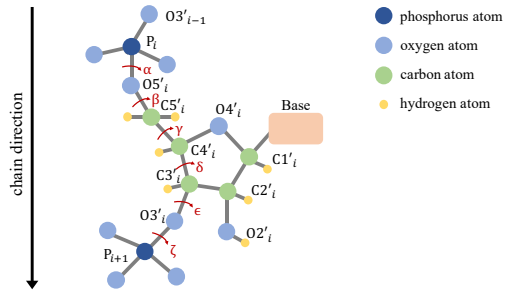


Figure 3: An example of structures in an RNA.

To adequately capture the complex structural information inherent in the three-dimensional folding of RNA molecules, we propose a general approach for modeling RNA tertiary structure. We represent RNA tertiary structure as an attributed graph $\mathcal{G} = (V, E)$ comprising node attributes V and edge attributes E . The graph is constructed by identifying the k nearest neighbors in 3D space for each node; each node i has a set of k neighbors denoted $\mathcal{N}(i, K)$. Specifically, $V \in \mathbb{R}^{N \times f_n}$ contains f_n -dimensional node attributes for N nodes, and $E \in \mathbb{R}^{k \times f_m}$ contains f_m -dimensional edge attributes for each node's K neighbors. By default, we set $k = 30$.

We outline the attributes used in our modeling approach along with their corresponding illustrations in Table 1, which includes two levels of attributes: (i) intra-nucleotide level attributes describing the local geometry of each nucleotide as the node attribute V , and (ii) inter-nucleotide level attributes describing the relative geometry between nucleotides as the edge attribute E .

Intra-nucleotide level (1) The dihedral angles, shown as red arrows in Figure 3, are calculated. We represent the dihedral angles of the RNA backbone using sin and cos functions. (2) The spatial distances between the *other intra-nucleotide atoms* and the atom P_i are encoded into radial basis functions (RBFs). (3) The directions of the other intra-nucleotide atoms relative to the atom P_i are calculated with respect to the local coordinate system \mathbf{Q}_i .

Inter-nucleotide level (1) An orientation encoding $\mathbf{q}(\cdot)$ is calculated from the quaternion representation of the spatial rotation matrix $\mathbf{Q}_i^T \mathbf{Q}_j$. (2) The spatial distances between inter-nucleotide atoms from *neighboring nucleotides* and the atom P_i are encoded into radial basis functions (RBFs). (3) The directions of the other inter-nucleotide atoms relative to the atom P_i are calculated.

Table 1: The feature construction of RNA tertiary structure modeling.

Level	Feature	Illustration
Intra-nucleotide	Dihedral Angle	$\{\sin, \cos\} \times \{\alpha_i, \beta_i, \gamma_i, \delta_i, \epsilon_i, \zeta_i\}$
	Distance	$\left\{ \text{RBF}(\ \omega_i - P_i\) \mid \omega \in \{O5', C5', C4', C3', O3'\} \right\}$
	Direction	$\left\{ \mathbf{Q}_i^T \frac{\omega_i - P_i}{\ \omega_i - P_i\ } \mid \omega \in \{O5', C5', C4', C3', O3'\} \right\}$
Inter-nucleotide	Orientation	$\mathbf{q}(\mathbf{Q}_i^T \mathbf{Q}_j)$
	Distance	$\left\{ \text{RBF}(\ \omega_j - P_i\) \mid j \in \mathcal{N}(i, K), \omega \in \{O5', C5', C4', C3', O3'\} \right\}$
	Direction	$\left\{ \mathbf{Q}_i^T \frac{\omega_j - P_i}{\ \omega_j - P_i\ } \mid j \in \mathcal{N}(i, K), \omega \in \{O5', C5', C4', C3', O3'\} \right\}$

3.3 Hierarchical Data-efficient Representation Learning

Now that RNA tertiary structure has been adequately modeled, the remaining challenge is how to learn from scarce data in a data-efficient manner. The key motivation is explicitly imposing the inherent data relationships based on prior knowledge. We first use L layers of message-passing neural networks (MPNNs) to learn the node representation. Specifically, the l -th hidden layer of the i -th nucleotide is defined as follows:

$$\mathbf{h}_{V_i}^{(l)} = \text{MPNN}([\mathbf{h}_{E_{ij}}, \mathbf{h}_{V_i}^{(l-1)}, \sum_{j \in \mathcal{N}(i, k)} \mathbf{h}_{V_j}^{(l-1)}]), \quad (5)$$

where $\mathbf{h}_V^{(0)}$, \mathbf{h}_E are the embeddings of the intra-nucleotide and inter-nucleotide level features from the tertiary structure modeling, respectively. When generating the RNA sequence, a fully connected layer f maps the node representation $\mathbf{h}_{V_i}^{(L)}$ to the RNA sequence space: $f(\mathbf{h}_{V_i}^{(L)})$.

To enable data-efficient representation learning, we need additionally obtain the graph-level representation through the average pooling of the node representations $\mathbf{h}_G = \frac{1}{N} \sum_{i=1}^N \mathbf{h}_{V_i}^{(L)}$ and the corresponding projection $g(\mathbf{h}_G)$ by the projection $g: \mathbb{R} \rightarrow \mathbb{S}$ that projects the Euclidean space into the hyperspherical space.

We propose a hierarchical representation learning framework comprising cluster-level and confidence-aware sample-level representation learning, as shown in Figure 4. The cluster-level representation learning utilizes topological similarity between RNA structures. We obtain RNA structure clusters based on TM-score, which indicates structural similarity[97]. We define positive pairs as RNA data with similar topological structures that attract each other in the embedding space, while negative pairs with dissimilar topological structures repel each other. The cluster-level representation learning is defined as follows:

$$\mathcal{L}_{\text{cluster}} = - \sum_{p \in \mathcal{D}} \log \frac{\exp(g_p \cdot g_q / \tau)}{\sum_{g_k \in \{g_q\} \cup \mathcal{K}_c} \exp(g_p \cdot g_k / \tau)}, \quad (6)$$

where (g_p, g_q) is a positive pair that comes from the same structural cluster, \mathcal{K}_c is a set of negative samples for g_p identified by the cluster they belong to, and \mathcal{D} is the data set. We denote g_p as the graph representation projection of the p -th RNA sample for notational convenience.

The confidence-aware sample-level representation learning is designed to capture the microscopic intrinsic properties of RNA structures. The positive pairs are defined as a given RNA structure sample and its random perturbed structures. The perturbed structures are obtained by adding Gaussian noise to the experimentally determined coordinates. To prevent excessive deviation, we filter out the perturbed structures with low structural similarity (TM-score ≤ 0.45) and high structural deviation (RMSD ≥ 1.0). The RMSD also evaluates the confidence level of the perturbed data. Formally, the sample-level representation learning can be formulated as:

$$\mathcal{L}_{sample} = - \sum_{p \in \mathcal{D}} \gamma_{p,p'} \log \frac{\exp(g_p \cdot g_{p'}/\tau)}{\sum_{g_k \in \{g_p'\} \cup \mathcal{K}_s} \exp(g_p \cdot g_k/\tau)}, \quad (7)$$

where p' is the perturbed structure of the p -th RNA structure, and \mathcal{K}_s is simply defined as other samples apart from g_p . The confidence score $\gamma_{p,p'}$ is defined as $\exp^{-\text{RMSD}(p,p')}$ so that when $\text{RMSD}(p,p') \rightarrow 0$, the confidence approaches 1.

The cluster-level representation provides a coarse-grained embedding, capturing the global topological similarity between RNA structures. The confidence-aware sample-level representation provides intrinsic knowledge that is robust to minor experimental deviations. As shown in Figure 4, by constraining the limited data into the restricted hyperspherical space with imposed prior knowledge, the intrinsic relationships between data are explicitly modeled.

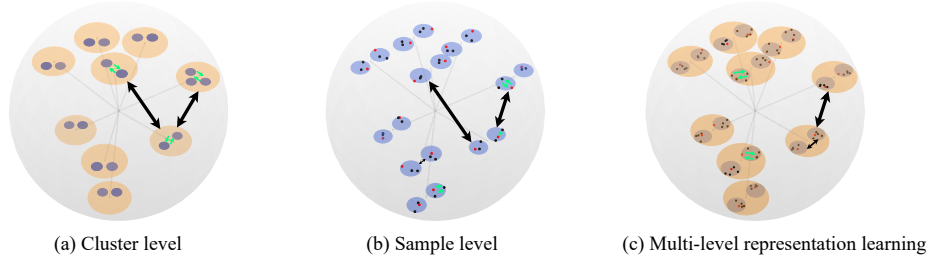


Figure 4: The different levels of hierarchical representation learning. Green arrows denote positive pairs tend to attract each other, and the black arrow denotes negative pairs tend to repel each other.

3.4 Secondary Structure Imposing Strategy

With the given tertiary structure, we can derive the corresponding secondary structure using the notation shown in Figure 2. The secondary structure is represented using parentheses to indicate paired nucleotides, with unpaired sites represented by one of the four RNA nucleotides (A, U, C, G). Paired sites are denoted by two nucleotides placed simultaneously in one of the following pairs: {CG, GC, AU, UA}. When a pair of positions (i, j) in the predicted primary sequence and its corresponding secondary structure are given, we can calculate the confidence score c_i for each position i based on the predicted letter at that position and the known secondary structure constraint. We then choose the position with the higher confidence score as the "reference" (say position i). We correct the predicted letter at the other position j so that the letters at positions i and j form one of the four allowed pairs.

Specifically, if position i is selected as the reference, we maintain the predicted letter at i unchanged and modify the predicted letter at j to satisfy the base pairing constraint. We then update the predicted primary sequence with this correction. By leveraging the information from the known secondary structure, we can rectify and refine the initially predicted primary sequence. The refinement helps enhance the accuracy of RNA 3D structure prediction. In the training phase, we compel the model to sharpen the confidence of the nucleotides in the paired positions. The supervised loss is defined as:

$$\mathcal{L}_{sup} = \sum_{(i,j) \in \text{Pairs}} \left[\ell_{CE}(s_i, f(\mathbf{h}_{V_i}^{(L)})/\tau') + \ell_{CE}(s_j, f(\mathbf{h}_{V_j}^{(L)})/\tau') \right] + \sum_{k \notin \text{Pairs}} \ell_{CE}(s_k, f(\mathbf{h}_{V_k}^{(L)})), \quad (8)$$

where Pairs encompasses all the paired position indices given by the secondary structure, τ' is the temperature that is set as 0.5 by default to sharpen the confidence of paired nucleotides.

Finally, the overall training objective is the linear combination of representation learning loss and supervised loss:

$$\mathcal{L} = \mathcal{L}_{sup} + \lambda(\mathcal{L}_{cluster} + \mathcal{L}_{sample}), \quad (9)$$

where we set the weight parameter λ as 0.5 by default.

4 Experiments

Datasets We evaluate our method on two tasks using three datasets: (i) We train and assess performance on our proposed RNA structure benchmark dataset, which aggregates and cleans data from RNAsolo [1] and the Protein Data Bank (PDB) [6, 7]. The benchmark dataset consists of 2216 RNA tertiary structures, which are divided into training (1772 structures), testing (223 structures), and validation (221 structures) sets based on their structural similarity. The RNA sequence length is highly consistent within each subset, minimizing negative effects from distribution shifts. (ii) To test the generalization ability, we apply pre-trained models to the Rfam [33, 32, 57, 57] and RNAPuzzle [55] datasets that contain non-overlapping structures. Rfam and RNAPuzzle are common datasets that contain novel RNA structures, which have 122 and 22 tertiary structures, respectively.

Metrics Previous protein design approaches usually use sequence perplexity and recovery metrics to evaluate the performance [49, 40, 84, 42, 74, 26, 59]. However, since RNA sequences only contain four letters, the perplexity metric traditionally used in natural language processing may not accurately reflect nucleotide-level prediction accuracy. Therefore, we use the recovery score to assess nucleotide-level accuracy by measuring the proportion of target RNA sequences that our model regenerates correctly. We also introduce the Macro-F1 score to evaluate performance by conceptualizing the RNA design task as a multi-class classification problem. The detailed illustrations of recovery and Macro-F1 scores are provided in Appendix ?? . We conducted each experiment three times with different random seeds and report the mean and standard deviation values.

Implementation Details In the experiments, we trained the model for 200 epochs using the Adam optimizer with a learning rate of 0.001. The batch size was set as 64. The model was implemented based on the standard PyTorch Geometric [22] library using the PyTorch 1.11.0 library. We ran the models on Intel(R) Xeon(R) Gold 6240R CPU @ 2.40GHz CPU and NVIDIA A100 GPU.

Baseline Models We explored five baseline models for RNA sequence design that could be categorized into three classes based on the level of structural information utilized: (i) Sequence-based models (SeqRNN and SeqLSTM) that do not utilize any structural information and could be viewed as the performance reference for RNA design; (ii) A structure-based model (StructMLP) that exploits structural features while ignoring the graph topological structure; (iii) Structure-based models (StructGNN and GraphTrans) [40] that incorporate the graph topological structure.

4.1 Standard Tertiary Structure-based RNA Design

Using our carefully curated benchmark dataset, we trained the model using the training set. Then, we evaluated the performance of the model on the testing set by selecting the model with the lowest loss on the validation set. Given that RNA sequences of varying lengths may impact prediction results, we stratified the testing set into three groups based on RNA length: (i) *Short*, RNA samples less than or equal to 50 nucleotides; (ii) *Medium* - RNA samples greater than 50 nucleotides but less than or equal to 100 nucleotides; (iii) *Long* - RNA samples greater than 100 nucleotides. To gain a thorough understanding of the relationship between RNA length and model accuracy, we reported both the recovery and Macro-F1 metrics for Short, Medium, and Long testing samples separately, in addition to overall testing set performance.

As presented in Table 2, the baseline models achieved suboptimal recovery scores, with performance ranging from 24-28%. Unexpectedly, tertiary structure-based models like StructMLP, StructGNN and GraphTrans attained comparable results to sequence-based models. This indicates that directly applying protein design techniques to RNA is misguided and fails to capture the intricacies of RNA structures. Moreover, StructMLP and GraphTrans achieved higher recovery scores for short RNA

Table 2: The recovery metric on the benchmark dataset. The best results are highlighted in bold.

Method	Short	Recovery (%) \uparrow		
		Medium	Long	All
SeqRNN (h=128)	26.52 \pm 1.07	24.86 \pm 0.82	27.31 \pm 0.41	26.23 \pm 0.87
SeqRNN (h=256)	27.61 \pm 1.85	27.16 \pm 0.63	28.71 \pm 0.14	28.24 \pm 0.46
SeqLSTM (h=128)	23.48 \pm 1.07	26.32 \pm 0.05	26.78 \pm 1.12	24.70 \pm 0.64
SeqLSTM (h=256)	25.00 \pm 0.00	26.89 \pm 0.35	28.55 \pm 0.13	26.93 \pm 0.93
StructMLP	25.72 \pm 0.51	25.03 \pm 1.39	25.38 \pm 1.89	25.35 \pm 0.25
StructGNN	27.55 \pm 0.94	28.78 \pm 0.87	28.23 \pm 1.95	28.23 \pm 0.71
GraphTrans	26.15 \pm 0.93	23.78 \pm 1.11	23.80 \pm 1.69	24.73 \pm 0.93
RDesign	38.79\pm1.71	44.27\pm0.89	44.02\pm0.73	41.69\pm0.76

sequences but struggle on longer, more complex RNA structures. Their struggles on the long dataset stem from the inability to learn from more intricate RNA structures and their low generalization capability. In contrast, our RDesign model outperforms all baseline methods on the recovery metric, achieving substantial gains. Specifically, RDesign attained a recovery rate of 41.69% on the testing set, demonstrating its superior ability to generate RNA sequences with higher fidelity than the baseline models. RDesign’s strong performance, particularly on medium and long sets, indicates that it can learn intrinsic RNA structural properties and generalize to complex structures.

Table 3: The Macro-F1 metric on the benchmark dataset. We multiply the score by 100 for aesthetics.

Method	Short	Macro F1 ($\times 100$) \uparrow		
		Medium	Long	All
SeqRNN (h=128)	17.22 \pm 1.69	17.20 \pm 1.91	8.44 \pm 2.70	17.74 \pm 1.59
SeqRNN (h=256)	12.54 \pm 2.94	13.64 \pm 5.24	8.85 \pm 2.41	13.64 \pm 2.69
SeqLSTM (h=128)	9.89 \pm 0.57	10.44 \pm 1.42	10.71 \pm 2.53	10.28 \pm 0.61
SeqLSTM (h=256)	9.26 \pm 1.16	9.48 \pm 0.74	7.14 \pm 0.00	10.93 \pm 0.15
StructMLP	17.46 \pm 2.39	18.57 \pm 3.45	17.53 \pm 8.43	18.88 \pm 2.50
StructGNN	24.01 \pm 3.62	22.15 \pm 4.67	26.05 \pm 6.43	24.87 \pm 1.65
GraphTrans	16.34 \pm 2.67	16.39 \pm 4.74	18.67 \pm 7.16	17.18 \pm 3.81
RDesign	38.21\pm4.59	42.51\pm4.31	41.48\pm7.38	42.29\pm0.24

It could be seen from Table 3 that there exist large gaps between the recovery metrics and Macro-F1 scores of most baseline models, which suggests those models tend to predict the high-frequency nucleotide letters instead of reflecting the actual tertiary structure. Among them, only StructGNN achieved consistent results in its Macro-F1 score and recovery metric but with unsatisfying performance. Our proposed RDesign consistently outperformed all other models on these metrics, demonstrating its effectiveness.

4.2 Evaluate the Generalization on Rfam and RNA-Puzzles

To rigorously assess the generalization capability of our model, we evaluated our model and the baseline methods on the Rfam [44] and RNA-Puzzles [55] datasets using the model pre-trained on our benchmark training set. We presented the results in Table 4. The performance remained consistent with that of our benchmark dataset. Specifically, StructGNN, which effectively learned certain tertiary structure information, achieved a relatively small gap between the recovery metric and Macro F1 score. In contrast, the other baselines that learned little structural information performed suboptimally. Our proposed RDesign model demonstrated superior generalization on both datasets and outperformed all the baselines by a considerable margin.

4.3 Ablation Study

We conducted an ablation study of our RDesign model and presented the results in Table 5. Firstly, we replaced our tertiary structure modeling approach with the classical modeling from protein design, which led to a significant decrease in performance. Secondly, removing the hierarchical representation

Table 4: The overall recovery and Macro-F1 scores on the Rfam and RNA-Puzzles datasets.

Method	Recovery (%) \uparrow		Macro F1 ($\times 100$) \uparrow	
	Rfam	RNA-Puzzles	RFam	RNA-Puzzles
SeqRNN (h=128)	27.99 \pm 1.21	28.99 \pm 1.16	15.79 \pm 1.61	16.06 \pm 2.02
SeqRNN (h=256)	30.94 \pm 0.41	31.25 \pm 0.72	13.07 \pm 1.57	13.24 \pm 1.25
SeqLSTM (h=128)	24.96 \pm 0.46	25.78 \pm 0.43	10.13 \pm 1.24	10.39 \pm 1.50
SeqLSTM (h=256)	31.45 \pm 0.01	31.62 \pm 0.20	11.76 \pm 0.08	12.22 \pm 0.21
StructMLP	24.40 \pm 1.63	24.22 \pm 1.28	16.79 \pm 4.01	16.40 \pm 3.28
StructGNN	27.64 \pm 3.31	27.96 \pm 3.08	24.35 \pm 3.45	22.76 \pm 3.19
GraphTrans	23.81 \pm 2.57	22.21 \pm 2.98	17.32 \pm 5.28	17.04 \pm 5.36
RDesign	58.25\pm0.92	50.57\pm0.81	55.03\pm0.93	47.06\pm0.60

learning also resulted in a performance drop, indicating its importance. In contrast, removing the secondary structure constraints provided a relatively small decrease in performance because RDesign itself could accurately generate RNA sequences.

Table 5: The ablation study of our model on three datasets.

Method	Recovery (%) \uparrow			Macro F1 ($\times 100$) \uparrow		
	Ours	Rfam	RNA-Puzzles	Ours	Rfam	RNA-Puzzles
RDesign	41.69	58.25	50.57	42.29	55.03	47.06
w/o our modeling	36.84	54.88	45.07	37.59	50.83	42.54
w/o representation learning	37.50	54.79	46.88	37.31	51.11	43.46
w/o secondary structure	39.06	56.96	48.29	39.95	53.04	45.94

We used RhoFold [69] to predict the structures of RNA sequences designed by RDesign. Figure 5 shows three visualization examples: (a) a short sequence that was easily reconstructed by RDesign; (b) a long sequence that was designed with a similar structure and low structure deviation; and (c) a complicated sequence that was designed with a similar structure but failed to achieve low structure deviation. These visualization examples demonstrate the effectiveness of our RDesign model in designing RNA sequences with structures similar to the target structure.

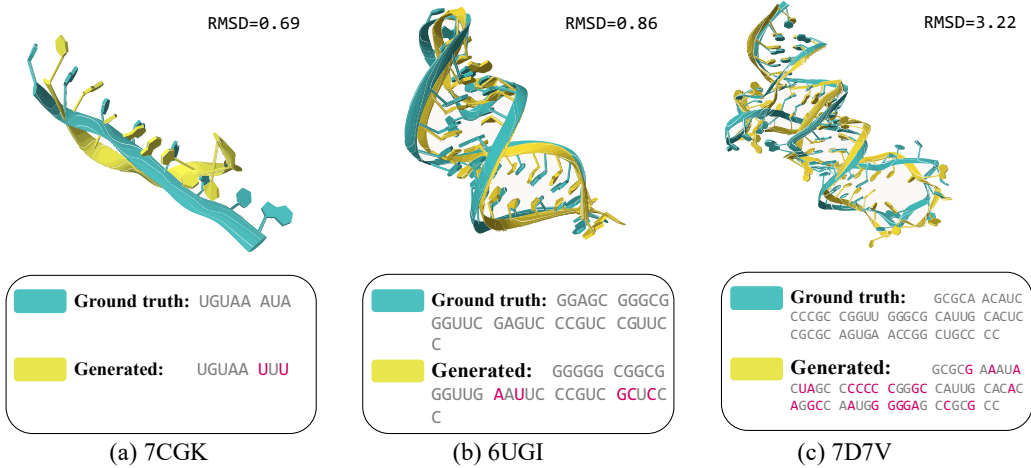


Figure 5: Visualization of RDesign’s designed examples.

5 Conclusion and Limitations

In this work, we investigate the challenging task of designing RNA tertiary structures. We compile a benchmark dataset to systematically assess the performance of various computational models on this

task. While existing protein design methods cannot be directly applied, we propose a hierarchical data-efficient representation learning framework. Our framework explicitly captures the intrinsic relationships within the data while constraining the limited data to a restricted hyperspherical space. We also introduce a secondary structure constraining strategy to leverage extra structural information. Extensive experiments demonstrate the effectiveness of our proposed RDesign model. We hope this work provides a new perspective on tertiary structure-based RNA design. A limitation is that our method is currently limited to in silico design we leave wet-lab validation to future work.

References

- [1] B. Adameczyk, M. Antczak, and M. Szachniuk. Rnasolo: a repository of cleaned pdb-derived rna 3d structures. *Bioinformatics*, 38(14):3668–3670, 2022.
- [2] M. Andronescu, A. P. Fejes, F. Hutter, H. H. Hoos, and A. Condon. A new algorithm for rna secondary structure design. *Journal of molecular biology*, 336(3):607–624, 2004.
- [3] C. Angermueller, T. Pärnamaa, L. Parts, and O. Stegle. Deep learning for computational biology. *Molecular systems biology*, 12(7):878, 2016.
- [4] M. Baek, F. DiMaio, I. Anishchenko, J. Dauparas, S. Ovchinnikov, G. R. Lee, J. Wang, Q. Cong, L. N. Kinch, R. D. Schaeffer, et al. Accurate prediction of protein structures and interactions using a three-track neural network. *Science*, 373(6557):871–876, 2021.
- [5] M. Baek, R. McHugh, I. Anishchenko, D. Baker, and F. DiMaio. Accurate prediction of nucleic acid and protein-nucleic acid complexes using rosettafoldna. *bioRxiv*, 2022.
- [6] P. D. Bank. Protein data bank. *Nature New Biol*, 233:223, 1971.
- [7] H. M. Berman, J. Westbrook, Z. Feng, G. Gilliland, T. N. Bhat, H. Weissig, I. N. Shindyalov, and P. E. Bourne. The protein data bank. *Nucleic acids research*, 28(1):235–242, 2000.
- [8] B. Bernstein, E. Birney, I. Dunham, E. Green, C. Gunter, and M. Snyder. Project consortium encode. *An integrated encyclopedia of DNA elements in the human genome. Nature*, 489:57–74, 2012.
- [9] A. Busch and R. Backofen. Info-rna—a fast approach to inverse rna folding. *Bioinformatics*, 22(15):1823–1831, 2006.
- [10] H. Cao, C. Tan, Z. Gao, G. Chen, P.-A. Heng, and S. Z. Li. A survey on generative diffusion model. *arXiv preprint arXiv:2209.02646*, 2022.
- [11] J. Chen, Z. Hu, S. Sun, Q. Tan, Y. Wang, Q. Yu, L. Zong, L. Hong, J. Xiao, T. Shen, et al. Interpretable rna foundation model from unannotated data for highly accurate rna structure and function predictions. *bioRxiv*, 2022.
- [12] S. Chen, Z. Sun, L. Lin, Z. Liu, X. Liu, Y. Chong, Y. Lu, H. Zhao, and Y. Yang. To improve protein sequence profile prediction through image captioning on pairwise residue distance map. *Journal of chemical information and modeling*, 60(1):391–399, 2019.
- [13] X. Chen, Y. Li, R. Umarov, X. Gao, and L. Song. Rna secondary structure prediction by learning unrolled algorithms. In *International Conference on Learning Representations*, 2019.
- [14] A. Churkin, M. D. Retwitzer, V. Reinharz, Y. Ponty, J. Waldispühl, and D. Barash. Design of rnas: comparing programs for inverse rna folding. *Briefings in bioinformatics*, 19(2):350–358, 2018.
- [15] F. Crick. Central dogma of molecular biology. *Nature*, 227(5258):561–563, 1970.
- [16] R. Das, J. Karanicolas, and D. Baker. Atomic accuracy in predicting and designing noncanonical rna structure. *Nature methods*, 7(4):291–294, 2010.
- [17] J. Dauparas, I. Anishchenko, N. Bennett, H. Bai, R. J. Ragotte, L. F. Milles, B. I. Wicky, A. Courbet, R. J. de Haas, N. Bethel, et al. Robust deep learning-based protein sequence design using proteinmpnn. *Science*, 378(6615):49–56, 2022.
- [18] I. Dotu, J. A. Garcia-Martin, B. L. Slinger, V. Mechery, M. M. Meyer, and P. Clote. Complete rna inverse folding: computational design of functional hammerhead ribozymes. *Nucleic acids research*, 42(18):11752–11762, 2014.
- [19] P. Eastman, J. Shi, B. Ramsundar, and V. S. Pande. Solving the rna design problem with reinforcement learning. *PLoS computational biology*, 14(6):e1006176, 2018.

- [20] J. W. Ellefson, J. Gollihar, R. Shroff, H. Shivram, V. R. Iyer, and A. D. Ellington. Synthetic evolutionary origin of a proofreading reverse transcriptase. *Science*, 352(6293):1590–1593, 2016.
- [21] E. Feingold and L. Pachter. The encode (encyclopedia of dna elements) project. *Science*, 306(5696):636–640, 2004.
- [22] M. Fey and J. E. Lenssen. Fast graph representation learning with pytorch geometric. *arXiv preprint arXiv:1903.02428*, 2019.
- [23] L. Fu, Y. Cao, J. Wu, Q. Peng, Q. Nie, and X. Xie. Ufold: fast and accurate rna secondary structure prediction with deep learning. *Nucleic acids research*, 50(3):e14–e14, 2022.
- [24] H. H. Gan, S. Pasquali, and T. Schlick. Exploring the repertoire of rna secondary motifs using graph theory; implications for rna design. *Nucleic acids research*, 31(11):2926–2943, 2003.
- [25] Z. Gao, Y. Hu, C. Tan, and S. Z. Li. Prefixmol: Target-and chemistry-aware molecule design via prefix embedding. *arXiv preprint arXiv:2302.07120*, 2023.
- [26] Z. Gao, C. Tan, S. Li, et al. Alphadesign: A graph protein design method and benchmark on alphafolddb. *arXiv preprint arXiv:2202.01079*, 2022.
- [27] Z. Gao, C. Tan, and S. Z. Li. Pifold: Toward effective and efficient protein inverse folding. *arXiv preprint arXiv:2209.12643*, 2022.
- [28] Z. Gao, C. Tan, and S. Z. Li. Diffds: A language diffusion model for protein backbone inpainting under geometric conditions and constraints. *arXiv preprint arXiv:2301.09642*, 2023.
- [29] Z. Gao, C. Tan, L. Wu, and S. Z. Li. Cosp: Co-supervised pretraining of pocket and ligand. *arXiv preprint arXiv:2206.12241*, 2022.
- [30] Z. Gao, C. Tan, L. Wu, and S. Z. Li. Semiretro: Semi-template framework boosts deep retrosynthesis prediction. *arXiv preprint arXiv:2202.08205*, 2022.
- [31] Z. Gao, C. Tan, L. Wu, and S. Z. Li. Simvp: Simpler yet better video prediction. In *Proceedings of the IEEE/CVF Conference on Computer Vision and Pattern Recognition*, pages 3170–3180, 2022.
- [32] P. P. Gardner, J. Daub, J. G. Tate, E. P. Nawrocki, D. L. Kolbe, S. Lindgreen, A. C. Wilkinson, R. D. Finn, S. Griffiths-Jones, S. R. Eddy, et al. Rfam: updates to the rna families database. *Nucleic acids research*, 37(suppl_1):D136–D140, 2009.
- [33] S. Griffiths-Jones, A. Bateman, M. Marshall, A. Khanna, and S. R. Eddy. Rfam: an rna family database. *Nucleic acids research*, 31(1):439–441, 2003.
- [34] R. Gstir, S. Schafferer, M. Scheideler, M. Misslinger, M. Griebel, N. Daschil, C. Humpel, G. J. Obermair, C. Schmuckermair, J. Striessnig, et al. Generation of a neuro-specific microarray reveals novel differentially expressed noncoding rnas in mouse models for neurodegenerative diseases. *Rna*, 20(12):1929–1943, 2014.
- [35] P. Guo, O. Coban, N. M. Snead, J. Trebley, S. Hoeprich, S. Guo, and Y. Shu. Engineering rna for targeted sirna delivery and medical application. *Advanced drug delivery reviews*, 62(6):650–666, 2010.
- [36] I. L. Hofacker. Vienna rna secondary structure server. *Nucleic acids research*, 31(13):3429–3431, 2003.
- [37] I. L. Hofacker, W. Fontana, P. F. Stadler, L. S. Bonhoeffer, M. Tacker, and P. Schuster. Fast folding and comparison of rna secondary structures. *Monatshefte für Chemie/Chemical Monthly*, 125(2):167–188, 1994.
- [38] C. Hsu, R. Verkuil, J. Liu, Z. Lin, B. Hie, T. Sercu, A. Lerer, and A. Rives. Learning inverse folding from millions of predicted structures. *bioRxiv*, 2022.
- [39] B. Hu, J. Xia, J. Zheng, C. Tan, Y. Huang, Y. Xu, and S. Z. Li. Protein language models and structure prediction: Connection and progression, 2022.
- [40] J. Ingraham, V. Garg, R. Barzilay, and T. Jaakkola. Generative models for graph-based protein design. *Advances in neural information processing systems*, 32, 2019.

- [41] M. Jeschek, R. Reuter, T. Heinisch, C. Trindler, J. Klehr, S. Panke, and T. R. Ward. Directed evolution of artificial metalloenzymes for in vivo metathesis. *Nature*, 537(7622):661–665, 2016.
- [42] B. Jing, S. Eismann, P. Suriana, R. J. L. Townshend, and R. Dror. Learning from protein structure with geometric vector perceptrons. In *International Conference on Learning Representations*, 2020.
- [43] J. Jumper, R. Evans, A. Pritzel, T. Green, M. Figurnov, O. Ronneberger, K. Tunyasuvunakool, R. Bates, A. Žídek, A. Potapenko, et al. Highly accurate protein structure prediction with alphafold. *Nature*, 596(7873):583–589, 2021.
- [44] I. Kalvari, E. P. Nawrocki, N. Ontiveros-Palacios, J. Argasinska, K. Lamkiewicz, M. Marz, S. Griffiths-Jones, C. Toffano-Nioche, D. Gautheret, Z. Weinberg, et al. Rfam 14: expanded coverage of metagenomic, viral and microrna families. *Nucleic Acids Research*, 49(D1):D192–D200, 2021.
- [45] K. Kaushik, A. Sivadas, S. K. Vellarikkal, A. Verma, R. Jayarajan, S. Pandey, T. Sethi, S. Maiti, V. Scaria, and S. Sivasubbu. Rna secondary structure profiling in zebrafish reveals unique regulatory features. *BMC genomics*, 19(1):1–17, 2018.
- [46] R. Kleinkauf, T. Houwaart, R. Backofen, and M. Mann. antarna—multi-objective inverse folding of pseudoknot rna using ant-colony optimization. *BMC bioinformatics*, 16(1):1–7, 2015.
- [47] B. Knudsen and J. Hein. Pfold: Rna secondary structure prediction using stochastic context-free grammars. *Nucleic acids research*, 31(13):3423–3428, 2003.
- [48] J. Kortmann and F. Narberhaus. Bacterial rna thermometers: molecular zippers and switches. *Nature reviews microbiology*, 10(4):255–265, 2012.
- [49] Z. Li, Y. Yang, E. Faraggi, J. Zhan, and Y. Zhou. Direct prediction of profiles of sequences compatible with a protein structure by neural networks with fragment-based local and energy-based nonlocal profiles. *Proteins: Structure, Function, and Bioinformatics*, 82(10):2565–2573, 2014.
- [50] Z. Liu, Y. Yang, D. Li, X. Lv, X. Chen, and Q. Dai. Prediction of the rna tertiary structure based on a random sampling strategy and parallel mechanism. *Frontiers in Genetics*, page 2521, 2022.
- [51] R. Lorenz, S. H. Bernhart, C. Höner zu Siederdissen, H. Tafer, C. Flamm, P. F. Stadler, and I. L. Hofacker. Viennarna package 2.0. *Algorithms for molecular biology*, 6(1):1–14, 2011.
- [52] J. D. Martell, M. Yamagata, T. J. Deerinck, S. Phan, C. G. Kwa, M. H. Ellisman, J. R. Sanes, and A. Y. Ting. A split horseradish peroxidase for the detection of intercellular protein–protein interactions and sensitive visualization of synapses. *Nature biotechnology*, 34(7):774–780, 2016.
- [53] D. H. Mathews. Rna secondary structure analysis using rnastructure. *Current Protocols in Bioinformatics*, 46(1):12–6, 2014.
- [54] S. Meyer, J. Chappell, S. Sankar, R. Chew, and J. B. Lucks. Improving fold activation of small transcription activating rnas (stars) with rational rna engineering strategies. *Biotechnology and bioengineering*, 113(1):216–225, 2016.
- [55] Z. Miao, R. W. Adamiak, M. Antczak, M. J. Boniecki, J. Bujnicki, S.-J. Chen, C. Y. Cheng, Y. Cheng, F.-C. Chou, R. Das, et al. Rna-puzzles round iv: 3d structure predictions of four ribozymes and two aptamers. *RNA*, 26(8):982–995, 2020.
- [56] T. Nagamune. Biomolecular engineering for nanobio/bionanotechnology. *Nano convergence*, 4(1):1–56, 2017.
- [57] E. P. Nawrocki, S. W. Burge, A. Bateman, J. Daub, R. Y. Eberhardt, S. R. Eddy, E. W. Floden, P. P. Gardner, T. A. Jones, J. Tate, et al. Rfam 12.0: updates to the rna families database. *Nucleic acids research*, 43(D1):D130–D137, 2015.
- [58] R. Nicholas and M. Zuker. Unafold: Software for nucleic acid folding and hybridization. *Bioinformatics*, 453:3–31, 2008.

- [59] J. O’Connell, Z. Li, J. Hanson, R. Heffernan, J. Lyons, K. Paliwal, A. Dehzangi, Y. Yang, and Y. Zhou. Spin2: Predicting sequence profiles from protein structures using deep neural networks. *Proteins: Structure, Function, and Bioinformatics*, 86(6):629–633, 2018.
- [60] R. Pearce, G. S. Omenn, and Y. Zhang. De novo rna tertiary structure prediction at atomic resolution using geometric potentials from deep learning. *bioRxiv*, 2022.
- [61] G. C. Pugh, J. R. Burns, and S. Howorka. Comparing proteins and nucleic acids for next-generation biomolecular engineering. *Nature Reviews Chemistry*, 2(7):113–130, 2018.
- [62] Y. Qi and J. Z. Zhang. Denscpd: improving the accuracy of neural-network-based computational protein sequence design with densenet. *Journal of chemical information and modeling*, 60(3):1245–1252, 2020.
- [63] M. Qin, Z. Liu, D. Li, X. Chen, X. Lv, X. Li, J. Zhou, and H. Wang. Improved predictive algorithm of rna tertiary structure based on gnn. In *2022 18th International Conference on Computational Intelligence and Security (CIS)*, pages 117–121. IEEE, 2022.
- [64] L. Rosenbaum. Tragedy, perseverance, and chance—the story of car-t therapy. *N Engl J Med*, 377(14):1313–1315, 2017.
- [65] A. Roth and R. R. Breaker. The structural and functional diversity of metabolite-binding riboswitches. *Annual review of biochemistry*, 78:305, 2009.
- [66] K. Rother, M. Rother, M. Boniecki, T. Puton, and J. M. Bujnicki. Rna and protein 3d structure modeling: similarities and differences. *Journal of molecular modeling*, 17:2325–2336, 2011.
- [67] F. Runge, D. Stoll, S. Falkner, and F. Hutter. Learning to design rna. In *International Conference on Learning Representations*, 2018.
- [68] K. Sato, M. Hamada, K. Asai, and T. Mituyama. Centroidfold: a web server for rna secondary structure prediction. *Nucleic acids research*, 37(suppl_2):W277–W280, 2009.
- [69] T. Shen, Z. Hu, Z. Peng, J. Chen, P. Xiong, L. Hong, L. Zheng, Y. Wang, I. King, S. Wang, et al. E2efold-3d: End-to-end deep learning method for accurate de novo rna 3d structure prediction. *arXiv preprint arXiv:2207.01586*, 2022.
- [70] J. Singh, J. Hanson, K. Paliwal, and Y. Zhou. Rna secondary structure prediction using an ensemble of two-dimensional deep neural networks and transfer learning. *Nature communications*, 10(1):1–13, 2019.
- [71] J. Singh, K. Paliwal, J. Singh, and Y. Zhou. Rna backbone torsion and pseudotorsion angle prediction using dilated convolutional neural networks. *Journal of Chemical Information and Modeling*, 61(6):2610–2622, 2021.
- [72] M. F. Sloma and D. H. Mathews. Exact calculation of loop formation probability identifies folding motifs in rna secondary structures. *RNA*, 22(12):1808–1818, 2016.
- [73] C. Tan, Z. Gao, S. Li, Y. Xu, and S. Z. Li. Temporal attention unit: Towards efficient spatiotemporal predictive learning. *arXiv preprint arXiv:2206.12126*, 2022.
- [74] C. Tan, Z. Gao, and S. Z. Li. Rfold: Towards simple yet effective rna secondary structure prediction. *arXiv preprint arXiv:2212.14041*, 2022.
- [75] C. Tan, Z. Gao, and S. Z. Li. Simvp: Towards simple yet powerful spatiotemporal predictive learning. *arXiv preprint arXiv:2211.12509*, 2022.
- [76] C. Tan, Z. Gao, and S. Z. Li. Target-aware molecular graph generation. *arXiv preprint arXiv:2202.04829*, 2022.
- [77] C. Tan, Z. Gao, and S. Z. Li. Protein complex invariant embedding with cross-gate mlp is a one-shot antibody designer, 2023.
- [78] C. Tan, Z. Gao, L. Wu, S. Li, and S. Z. Li. Hyperspherical consistency regularization. In *Proceedings of the IEEE/CVF Conference on Computer Vision and Pattern Recognition*, pages 7244–7255, 2022.
- [79] C. Tan, Z. Gao, J. Xia, and S. Z. Li. Generative de novo protein design with global context. *arXiv preprint arXiv:2204.10673*, 2022.
- [80] C. Tan, J. Xia, L. Wu, and S. Z. Li. Co-learning: Learning from noisy labels with self-supervision. In *Proceedings of the 29th ACM International Conference on Multimedia*, pages 1405–1413, 2021.

- [81] R. J. Townshend, S. Eismann, A. M. Watkins, R. Rangan, M. Karelina, R. Das, and R. O. Dror. Geometric deep learning of rna structure. *Science*, 373(6558):1047–1051, 2021.
- [82] A. Vaswani, N. Shazeer, N. Parmar, J. Uszkoreit, L. Jones, A. N. Gomez, Ł. Kaiser, and I. Polosukhin. Attention is all you need. *Advances in neural information processing systems*, 30, 2017.
- [83] M. Wachsmuth, S. Findeiß, N. Weissheimer, P. F. Stadler, and M. Mörl. De novo design of a synthetic riboswitch that regulates transcription termination. *Nucleic acids research*, 41(4):2541–2551, 2013.
- [84] J. Wang, H. Cao, J. Z. Zhang, and Y. Qi. Computational protein design with deep learning neural networks. *Scientific reports*, 8(1):1–9, 2018.
- [85] J. Wang and N. V. Dokholyan. Application of rna tertiary structure prediction tool ifoldrna in rna nanotechnology. In *RNA Nanotechnology and Therapeutics*, pages 101–109. CRC Press, 2022.
- [86] P. H. Wanrooij, J. P. Uhler, T. Simonsson, M. Falkenberg, and C. M. Gustafsson. G-quadruplex structures in rna stimulate mitochondrial transcription termination and primer formation. *Proceedings of the National Academy of Sciences*, 107(37):16072–16077, 2010.
- [87] K. D. Warner, C. E. Hajdin, and K. M. Weeks. Principles for targeting rna with drug-like small molecules. *Nature reviews Drug discovery*, 17(8):547–558, 2018.
- [88] J. Xia, G. Wang, B. Hu, C. Tan, J. Zheng, Y. Xu, and S. Z. Li. Wordreg: Mitigating the gap between training and inference with worst-case drop regularization. In *ICASSP 2023-2023 IEEE International Conference on Acoustics, Speech and Signal Processing (ICASSP)*, pages 1–5. IEEE, 2023.
- [89] J. Xia, C. Zhao, B. Hu, Z. Gao, C. Tan, Y. Liu, S. Li, and S. Z. Li. Mole-bert: Rethinking pre-training graph neural networks for molecules. 2023.
- [90] J. Xia, J. Zheng, C. Tan, G. Wang, and S. Z. Li. Towards effective and generalizable fine-tuning for pre-trained molecular graph models. *bioRxiv*, 2022.
- [91] P. Xiong, R. Wu, J. Zhan, and Y. Zhou. Pairing a high-resolution statistical potential with a nucleobase-centric sampling algorithm for improving rna model refinement. *Nature communications*, 12(1):1–11, 2021.
- [92] Y. Xu, Z. Zang, J. Xia, C. Tan, Y. Geng, and S. Z. Li. Structure-preserving visualization for single-cell rna-seq profiles using deep manifold transformation with batch-correction. *Communications Biology*, 6(1):369, 2023.
- [93] X. Yang, K. Yoshizoe, A. Taneda, and K. Tsuda. Rna inverse folding using monte carlo tree search. *BMC bioinformatics*, 18(1):1–12, 2017.
- [94] J. D. Yesselman and R. Das. Rna-redesign: a web server for fixed-backbone 3d design of rna. *Nucleic Acids Research*, 43(W1):W498–W501, 2015.
- [95] J. N. Zadeh, C. D. Steenberg, J. S. Bois, B. R. Wolfe, M. B. Pierce, A. R. Khan, R. M. Dirks, and N. A. Pierce. Nupack: Analysis and design of nucleic acid systems. *Journal of computational chemistry*, 32(1):170–173, 2011.
- [96] Y. Zhang, Y. Chen, C. Wang, C.-C. Lo, X. Liu, W. Wu, and J. Zhang. Prodconn: Protein design using a convolutional neural network. *Proteins: Structure, Function, and Bioinformatics*, 88(7):819–829, 2020.
- [97] Y. Zhang and J. Skolnick. Tm-align: a protein structure alignment algorithm based on the tm-score. *Nucleic acids research*, 33(7):2302–2309, 2005.
- [98] J. Zheng, S. Li, C. Tan, C. Wu, Y. Chen, and S. Z. Li. Leveraging graph-based cross-modal information fusion for neural sign language translation. *arXiv preprint arXiv:2211.00526*, 2022.
- [99] J. Zheng, G. Wang, Y. Huang, B. Hu, S. Li, C. Tan, X. Fan, and S. Z. Li. Lightweight contrastive protein structure-sequence transformation. *arXiv preprint arXiv:2303.11783*, 2023.
- [100] J. Zheng, Y. Wang, C. Tan, S. Li, G. Wang, J. Xia, Y. Chen, and S. Z. Li. Cvt-slr: Contrastive visual-textual transformation for sign language recognition with variational alignment. *arXiv preprint arXiv:2303.05725*, 2023.

- [101] M. Zuker. Mfold web server for nucleic acid folding and hybridization prediction. *Nucleic acids research*, 31(13):3406–3415, 2003.